Structure of boron nitride nanoscale cones: Ordered stacking of 240° and 300° disclinations

L. Bourgeois,* Y. Bando, W. Q. Han,† and T. Sato
National Institute for Research in Inorganic Materials, Namiki 1-1, Tsukuba Ibaraki 305-0044, Japan
(Received 24 September 1999)

Recently discovered boron nitride (BN) nanoscale cone particles are shown to consist of an ordered stacking of seamless conical shells. High-resolution transmission electron microscopy and nanobeam electron diffraction allowed the orientation of the BN hexagonal rings to be determined. In all but one case, the results conformed with a model of orderly stacked 240° disclinations, which is the smallest cone geometry ensuring the presence of B-N bonds only. One case of a nanoscale cone constituted of 300° disclinations was found, implying that structures containing line defects of non-B-N bonds may form.

I. INTRODUCTION

Cones are interesting because their departure from a flat surface can be solely determined by the topological defect located at their apex. For a two-dimensional lattice with hexagonal symmetry, as in graphitic carbon and trigonal boron nitride, the simplest such defects are pentagonal and square rings. A single one of these defects inserted into the hexagonal lattice will result in a cone whose apex angle is directly related to the size of the ring. Ring defects larger than hexagons (e.g., heptagons) will not generate cones, but saddle-shaped surfaces. A cone's apex may also consist of a combination of ring defects. However complicated this combination may be, for a two-dimensional array with discrete symmetry elements, there will only be a discrete number of possible apex angles. This can be understood by realizing that a cone can be obtained through the operation where a sector of angle D_θ (the disclination angle) is removed from a flat sheet, and the two cut sides of the sheet are joined together. Continuity at the junction is only satisfied if D_θ takes certain values. A cone can then be defined by its disclination angle, although this does not always allow a unique determination of the apical defects.

Ring defects are necessary to the emergence of curvature in layered structures on the nanometric scale. This was suggested some time ago for microporous carbon, a highly disordered material.[1] More recently, it was found that an ordered arrangement of some specific ring defects within a hexagonal lattice would lead to closed cage structures, the simplest and most famous one of them being the fullerene C_{60}.[2] In C_{60} the defects are pentagons, of which there are twelve. In boron nitride (BN) however, even-membered rings, and in particular squares, are thought to be the preferred defects because they do not necessitate the inclusion of B-B or N-N bonds, which are weaker than B-N bonds.[3,4] The presence of odd-membered rings becomes more and more costly the larger the shell, as line defects of B-B or N-N bonds between ring-defects become longer.[5] The common occurrence of flat caps — presumably constructed from three squares — in BN nanotubes,[5] the more faceted appearance of BN shells produced by electron beam irradiation[6] and the sharper tips exhibited by BN helical cones compared with C cones[7] indicate that squares are indeed the favored ring defects in BN. Nevertheless, there is still some degree of uncertainty as to whether BN square rings can readily nucleate and lead to the formation of fullerene cages. For example, the difficulty with which BN shells form under electron irradiation has been interpreted by some authors[8] as showing that two dimensionally curved surfaces of BN are not energetically stable, in contrast with carbon where they easily form.[9] Yet the fabrication of BN fullerene analogs would be an important extension of the concept of perfectly closed cages of atoms. Until now, the only system other than carbon which has been observed to exhibit perfect fullerene geometry is MoS_2.[10] It is therefore of significant interest to estimate the stability of ring defects in BN.

Conical morphologies have been observed for a variety of layered materials: graphite,[11] BN (Ref. 12), and aluminosilicates.[13,14] Despite the fact that these particles are helical, i.e., that they consist of a single conical layer wrapped helically about the cone axis, information about the nucleation of ring defects could be obtained (see Ref. 15 for C, and Ref. 16 for BN). These results were confirmed in a transmission electron microscopy study where the morphologies of coproduced BN and C helical cones were compared: C cones had apex angles compatible with pentagonlike apical defect, whereas BN exhibited sharper tips more consistent with a squarelike apical defect.[7] The helical nature of the particles meant that the ring defects were not closed. In this paper, unambiguous evidence of the existence of seamless conical BN shells is presented. This follows an initial report by the authors of the discovery of BN nanoscale cones, where apex angles were always observed to be very close to the 38.9° value for a 240° disclination.[17] A 240° disclination is one of five possibilities for a sheet of trigonal symmetry. Here, it is shown that the nanoscale cones are indeed perfect 240° disclinations. A 300° disclination was also found, suggesting that odd-membered rings, and more importantly, line defects of non-B-N bonds, may form in BN.

II. EXPERIMENTAL DETAILS

The nanoscale cones are part of a material constituted primarily of BN nanotubes.[17] The material was synthesized by reacting boron oxide vapor with chemically vapor-deposited carbon nanotubes under the flow of nitrogen, at 1500 °C.[18] Observations were carried out on a JEOL 3000F field-emission high-resolution transmission electron microscope (HRTEM) operated at 300 kV and equipped with a

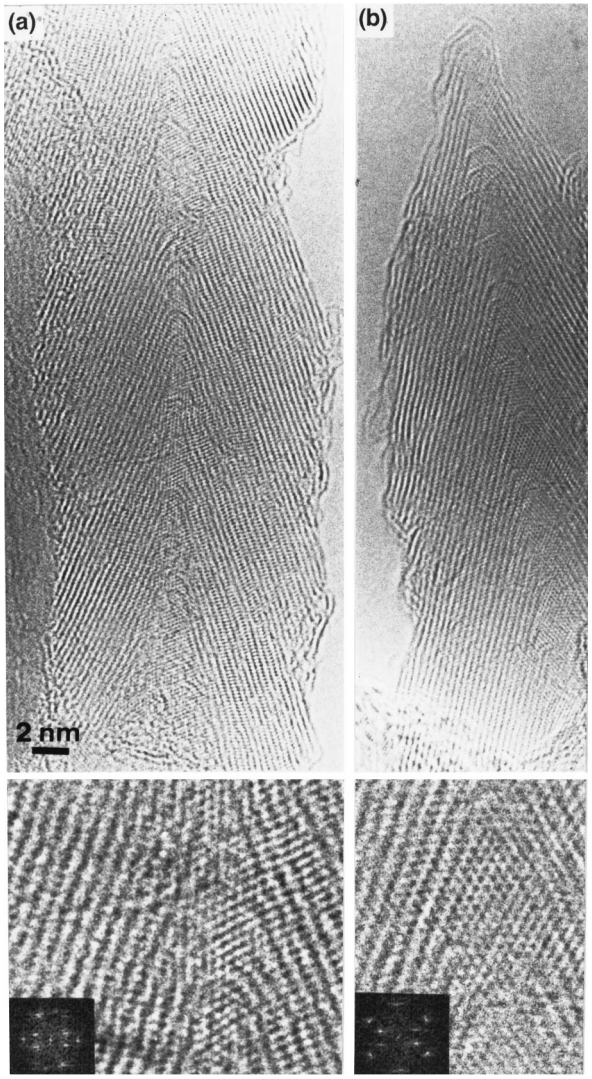

FIG. 1. High-resolution transmission electron micrographs of two BN nanoscale cone particles with apex angles close to 39°. Enlargements of the core regions exhibit hexagonal fringe patterns, each dot representing a BN hexagon; taking the fast Fourier transform of these regions (see insets) gives the orientation of the BN hexagons with respect to the cone axis: zigzag orientation in (a), and armchair orientation in (b).

$\pm 30°$ double-tilt stage. Electron diffraction of the particles was performed with a 1.6-nm diameter beam. The image simulations are multi slice calculations done with the MacTempas software, and fast Fourier transforms of the HRTEM images were computed with the DigitalMicrograph software.

III. RESULTS

In Fig. 1, HRTEM micrographs of two typical nanoscale cone particles are shown. The nanoscale cones consist of slanted walls approximately 10 nm in width separated by a thin, possibly empty core (diameter ≈ 1 nm). The observed apex angle (i.e., the angle measured on the image) is $42 \pm 1°$ in both cases. This is fairly close to the theoretical value of 38.9° for the apex angle of a 240° disclination.[17] The value of 240° is one of two cases (with 120°) ensuring continuity of the BN hexagonal lattice along the entire surface of the cone. For carbon the possibilities increase to five (disclination angle $D_\theta = 60°, 120°, \ldots, 300°$), which correspond to apex angles $\theta_{apex} = 2a \sin(1 - D_\theta/360) = 112.9°$, $83.6°, \ldots, 19.2°$, respectively.[19] Therefore the type of disclination observed here, with $D_\theta = 240°$, is consistent with the symmetry requirement for BN. Such a 240° disclination is sketched in Fig. 2. Note that the apex is shown to consist of two hexagons sharing a B-N bond, i.e., the apical defect is a single two-membered ring. This kind of defect is probably highly unstable as a result of the large strain associated with non-120° bond angles. More likely configurations will be discussed later. Two different orientations about the cone axis are shown in Fig. 2. As the conical sheet is rotated about its disclination axis, the hexagons of a given surface element rotate about their local normal. For a 240° disclination there are four orientations, 90° apart, where hexagons from opposite sides of the cone will be the mirror image of each other, the mirror plane being parallel to the viewing plane and containing the disclination axis. Figure 2 shows the cone near two of these positions. In Fig. 2(a), the hexagons which are more or less parallel to the viewing plane are in the zigzag orientation, whereas in Fig. 2(b) they are in the armchair orientation. In Fig. 3 the cone of Fig. 2 is rotated about the cone axis and set in an arbitrary orientation, which is measured by the angle ϕ. $\phi = 0$ is defined to correspond to the zigzag position, and $\phi = \phi_a$ as the direction normal to the viewing plane and intersecting the cone axis. Since the particle is viewed normal to its cone axis, atoms from opposite sides of the cone, near the ϕ_a direction, will appear mirror of each other relative to the cone axis. This is a characteristic of 240° and 120° disclinations only, and reflects the fact that they exhibit twofold and fourfold symmetry, respectively (if one makes abstraction of the difference between B and N atoms, which cannot be detected by elastic scattering of the electron beam and therefore does not manifest itself in the diffraction patterns or the high-resolution images). If the cone axis is not exactly parallel to the viewing plane, as will often be the case during TEM observations, the mirror symmetry between hexagons from opposite sides of the cone will still be apparent, albeit approximately. Tilting of up to 20° was found to preserve this feature.

Enlargements of the core region of the particles in Fig. 1 reveal hexagonal fringe patterns exhibiting the same orientations with respect to the cone axis as those shown in Fig. 2. Furthermore, observation of such two-dimensional fringe patterns for a number of other nanoscale cones always corresponded with hexagons in one of the two orientations of Fig. 2; in many cases no clear fringe patterns could be found in the particles' core, which was probably the result of the arbitrary orientation of the cones about their axis. Therefore, it may be suggested that the nanoscale cones of Fig. 1 are 240° disclinations seen along the two different directions shown in Fig. 2.

In order to give more weight to this claim, nanobeam electron diffraction (NBD) patterns were taken for all observed particles. The electron beam was focused onto the cone axis, in an almost normal position (i.e., with the projected apex angle close to its minimum value). This allowed probing of the local orientation of the hexagons along the path of the electron beam and hence, indirectly, of the sym-

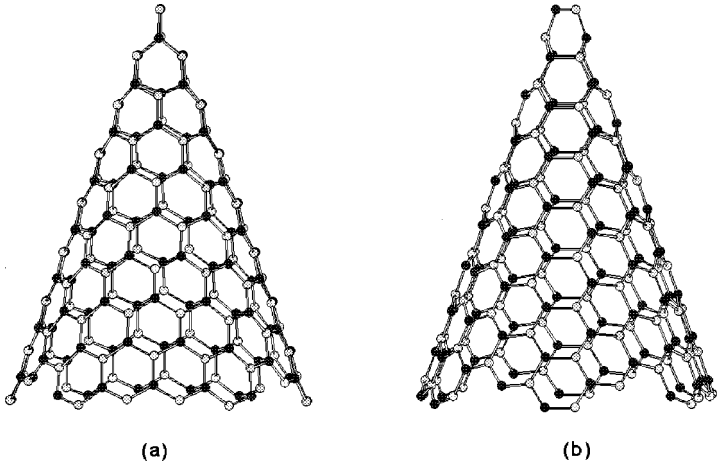

FIG. 2. A 240° disclination, i.e., a cone with apex angle 38.9°, for BN. The only defect is a two-membered ring at the apex. Two orientations of the cone about its disclination axis are shown: so that the hexagons of the surface element perpendicular to the viewing direction are in the zigzag orientation (a), and in the armchair configuration (b). The two positions are separated by a 90° rotation about the cone axis.

metry of the disclination axis. NBD patterns taken for the nanoscale cones of Figs. 1(a) and 1(b) are presented in Figs. 4(a) and 4(b), respectively. Common to these diffraction patterns are the following features. First, two g_{002} reflections (g_{002} is the scattering vector corresponding to the layer periodicity $d_{002}=3.42$ Å) separated by an angle equal to θ_{obs}. They are caused by scattering from the two opposite sides of the cone's walls, which are parallel to the incoming electron beam. The two faint spots with $|g_{002}|$ magnitude in Figs. 4(a) and 4(b) are spurious reflections. The cone axis is perpendicular to the median of the two $002/00\bar{2}$ rows (defined as the line M in the figures). Second, and most importantly, two sets of hexagonal $|g_{100}|$ reflections mirror of each other through M. These spots are located in positions consistent with the hexagonal fringe patterns observed in the high-resolution images: zigzag orientation in Figs. 1(a) and 2(a), and armchair orientation in Figs. 1(b) and 2(b). The existence of two sets of hexagonal diffraction spots symmetrical about the cone axis can be taken as strong indication that the nanoscale cones possess twofold symmetry and are therefore 240° disclinations. From the NBD patterns it is indeed clear that the particles are composed of individual seamless cones

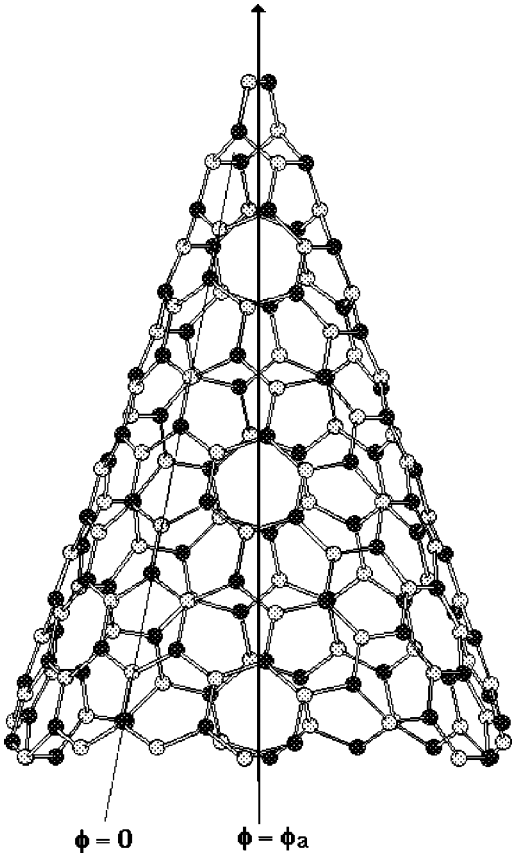

FIG. 3. Arbitrary rotation angle of the cone about its disclination axis: for a 240° disclination, the cone axis (arrow) is a twofold symmetry axis.

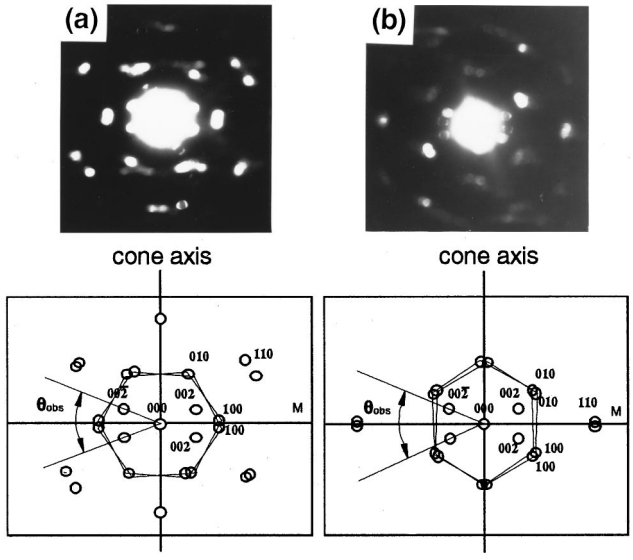

FIG. 4. Electron diffraction patterns taken with a nanobeam probe (nominally 1.6 nm in diameter) very close to the cone axis for the two particles of Fig. 1, respectively. Explanatory sketches of the diffraction spot patterns are included. The fact that the cone axis is a mirror line confirms that the cones are 240° disclinations all in the same ϕ_a orientation.

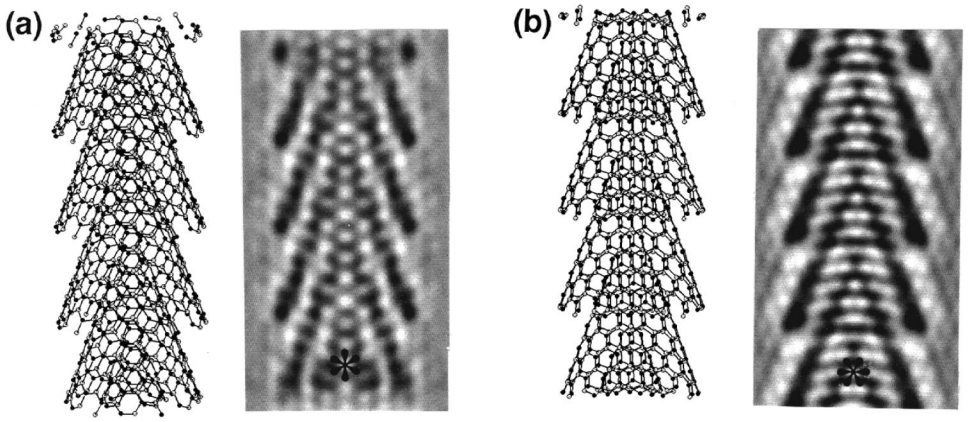

FIG. 5. Monolayer cones stacked on top of each other with the same ϕ orientations: $\phi_a = 10°$ in (a); $\phi_a = 80°$ in (b); both have their cone axis tilted by about 10° relative to the incoming electron beam. The interlayer distance is 3.42 Å, that of turbostratic BN. Despite the fact that there are very few coincidental lattice sites, hexagonal fringe patterns are visible in the simulated images (as indicated by six-branch star).

stacked on top of each other, and not of a helically wrapped conical sheet with disclination angle close to 240°. Since at least 30 conical layers contribute to each diffraction pattern (the cones' lateral size is 12 nm or larger), and that a helicity-caused overall rotation of the (hk0) spots greater than about 5° would be detected, the helicity must be less than about 0.17°. In our view, the existence of extremely small helicities for all investigated cones (about twenty) is highly unlikely, as relaxation of a helically wrapped monolayer of BN (or C) leads to a rather broad distribution of helicities.[7,20]

The presence of only two sets of reflections also indicates that individual conical monolayers making up the particles are aligned so as to have their orientation angle ϕ_a equal. This explains why hexagonal fringe patterns could often be observed in the nanoscale cone cores. Yet, when building structure models of cone stackings, one realizes that interlayer distances in the range 3.3–3.5 Å are not compatible with obtaining regions of hexagonal(h)-BN-like ordered stacking, even along the four zigzag and armchair orientation directions. Despite this lack of h-BN-like ordering, image simulations of cone models exhibiting the typical turbostratic BN interlayer distance of 3.42 Å, and with their constituent cone layers aligned in the same ϕ_a orientation (see Fig. 5) displayed hexagonal fringes when $\phi_a = 10°$ [Fig. 5(a)] or $\phi_a = 80°$ [Fig. 5(b)], and with the cone axis tilted by about 10° from the normal position relative to the incident electron beam. Larger cone stacking models could not be used in order to generate more realistic simulated images, and in particularly confirm whether dozens of conical layers overlapping in an ordered way would also produce clear hexagonal lattice fringes. However, a significant improvement in fringe definition was observed from a single cone to two superimposed cones; this is taken as sufficient evidence that alignment of individual cones is enough to result in the observed fringe patterns, without the intervention of polygonization and local h-BN-like ordering.

Returning to Fig. 4, a more accurate assessment of the mirror relationship expressed by the hexagonal sets of reflections shows that it holds very well when the diffraction spots (g_{100} or g_{110}) are close to M, but does not always do so for reflections closer to the cone axis [see Fig. 4(a)]. This is probably a result of the viewing direction not being perpendicular to the cone axis, an effect likely to be particularly strong due to the steep slope of the disclinations. Tilting of the cone parallel to the viewing direction will strongly affect the direction of local (hk.0) scattering vectors positioned along the slope, but not that of (hk.0) vectors perpendicular to the slope. On the other hand, faceting of the nanoscale cones, observed for some particles seen almost along their cone axis, and sometimes manifested as slightly different (002) lattice fringe contrast on HRTEM images, would affect the symmetry relationship exhibited by all (hk.0) diffraction spots. This was not detected in the NBD patterns. Therefore it may be inferred that either faceting is minimal, or that it retains the two-fold symmetry characteristic of the 240° disclination.

As mentioned before, all but one of the twenty or so observed nanoscale cones exhibited features consistent with the model of 240° disclinations stacked in an ordered way. Figures 6(a)–6(b) show HRTEM images and NBD of this exception. The projected apex angle measured on the images is 20°, which is only slightly larger than the value of 19.1° for a 300° disclination. Enlargement of the nanoscale cone's core [Fig. 6(b)] shows hexagonal dots in an orientation that is different from that observed for all 240° disclinations. This is confirmed by the diffraction pattern. A model for a 300° disclination [see Fig. 6(c)] in the orientation where opposite sides of the cone map each other presents hexagons in exactly the same arrangement as observed experimentally. Again, this brings strong support to the model of seamless conical shells stacked on top of each other in an ordered manner. A seamless 300° disclination for BN entails the presence of a line defect, consisting of B-B bonds presumably, since they are energetically preferable to N-N bonds [see Fig. 6(d)]. This result indicates that structures containing non-B-N bonds may form and remain stable, although they are less likely to do so than those containing B-N bonds only.

IV. DISCUSSION

It has been noted that the nanoscale cones all displayed a hollow or amorphous core surrounding the cone axis. In

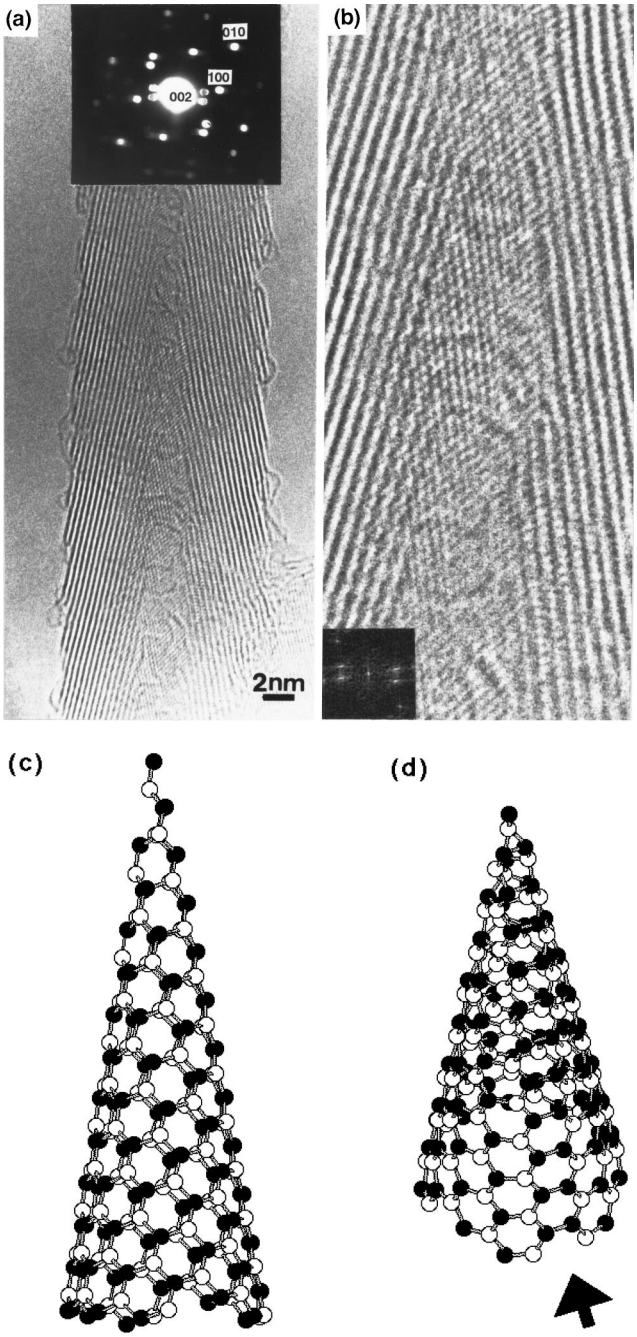

FIG. 6. (a) Nanoscale cone with projected apex angle measured to be 20°, which is close to the value of 19.2° for a 300° disclination. Enlargement of the core region (b) reveals hexagonal fringes oriented as one would expect for a 300° disclination in the orientation shown in (c). The nanobeam diffraction pattern inset in (a) is consistent with the high-resolution image and 300° disclination model. (d) shows the line defect consisting of like bonds.

some cases, [e.g., Fig. 1(b)] low-curvature ''bridges'' appear to join the two opposite sides of the cone's walls, but generally the apical region clearly seems empty or highly disordered. Since the formation of 240° disclinations results from the nucleation of one or several ring defects (two squares or four pentagons), it may be suggested that the apical region did exist early during the growth stage of the cones, but that excessive strain imposed by the growing size of the particles, and concentrated at the defective area, the apex, led to its breaking. All observed nanoscale cones exhibited a fairly uniform diameter of about 15 nm, and therefore this idea could not be tested by looking at whether smaller particles displayed an intact apex. Nonetheless, the high degree of order detected in the cones' structure provides strong indication that the ring-defect containing part of the shells was a stable configuration at the start of the growth process.

The ordered stacking of individual conical shells may seem surprising considering that, as has been pointed out, it is not possible to obtain the stacking arrangement typical of h-BN, even locally. On the other hand it is plausible that a 240° disclination will possess some degree of faceting near its apex, especially if it resulted from the nucleation of two squares (rather than four pentagons, where the strain would be more evenly distributed). Such faceting might cause ''locking'' of the cones' apexes into the same orientation, in order to allow greater interlayer interaction. Polygonization was found to be weak, if present at all. This indicates that there are no large areas with h-BN-like three-dimensional ordering, which in turns suggests that growth of additional layers started around the apical region.

The sole case of a 300° disclination amidst about twenty 240° disclinations confirms the preference for even-membered rings or even numbers of odd-membered rings in BN. Concurrently, it signifies that nucleation of an odd number of pentagons has a non-negligible probability, and that the subsequent development of a line defect of non-B-N bonds may lead to an apparently stable structure. In contrast, C nanoscale cones synthesized in conjunction with C nanotubes are almost always 300° disclinations.[21] Interestingly, the ratio of BN cone numbers between the unfavored and the favored configurations is roughly the same ($\approx$20%) for nanoscale cones and for helical cones.[7,16] These figures should be taken with caution due to the small size of the statistical sample. Moreover the nucleation and growth conditions of the two types of cones are very different. Nevertheless, these results point to a fundamental property of the BN system: squares and pentagons can lead to stable nanostructures. Consequently, it should be expected that BN fullerenes will be successfully synthesized in the near future, despite the fact that the slightly more complicated structure of BN compared with carbon means it is more difficult to find the appropriate kinetical conditions.

V. CONCLUSION

BN nanoscale cones were determined to consist of conical monolayers corresponding to disclinations of integral numbers of 120°. In all but one case, the disclination angle was 240°, the smallest value compatible with preservation of the BN lattice's symmetry. Observation of a nanoscale cone particle comprised of 300° disclinations suggested that the requirement that only B-N bonds should form is not so stringent energetically.

ACKNOWLEDGMENTS

The authors wish to acknowledge Dr. D. Golberg for making helpful suggestions. L. B. is grateful for the support of the Science and Technology Agency.

*Author to whom correspondance should be addressed. Electronic address: laure@nirim.go.jp
†Present address: Max-Planck-Institut für Metallforschung, Seestr. 92 Stuttgart, D-70174, Germany.

[1] S. Iijima, J. Microsc. **119**, 99 (1980); J. Cryst. Growth **50**, 675 (1980).
[2] H. W. Kroto, J. R. Health, S. C. O'Brien, R. F. Curl, and R. E. Smalley, Nature (London) **318**, 162 (1985).
[3] F. Jensen and H. Toftlund, Chem. Phys. Lett. **201**, 89 (1993).
[4] G. Seifert, P. W. Fowler, D. Mitchell, D. Poregaz, and Th. Frauenheim, Chem. Phys. Lett. **268**, 352 (1997).
[5] A. Loiseau, F. Willaime, N. Demoncy, G. Hug, and H. Pascard, Phys. Rev. Lett. **76**, 4737 (1996).
[6] O. Stéphan, Y. Bando, A. Loiseau, F. Willaime, N. Shramchenko, T. Tamiya, and T. Sato, Appl. Phys. A: Mater. Sci. Process. **67**, 108 (1998); D. Golberg, Y. Bando, O. Stéphan, and K. Kurashima, Appl. Phys. Lett. **73**, 2441 (1998).
[7] L. Bourgeois, Y. Bando, K. Kurashima, and T. Sato, Philos. Mag. A **80**, 129 (2000).
[8] F. Banhart, M. Zwanger, and H.-J. Muhr, Chem. Phys. Lett. **231**, 98 (1994).
[9] D. Ugarte, Nature (London) **359**, 707 (1992).
[10] P. A. Parilla, A. C. Dillon, K. M. Jones, G. Riker, D. L. Schultz, D. S. Ginley, and M. J. Heben, Nature (London) **397**, 114 (1999).
[11] H. B. Haanstra, W. F. Knippenberg, and G. Verspui, J. Cryst. Growth **16**, 71 (1972).
[12] T. Sato, NIRIM Research Report (unpublished), Vol. 89, Chap. 3, pp. 17–23.
[13] K. Yada, Acta Crystallogr., Sect. A: Cryst. Phys., Diffr., Theor. Gen. Crystallogr. **27**, 659 (1971).
[14] S. Amelinckx, B. Devouard, and A. Baronnet, Acta Crystallogr., Sect. A: Found. Crystallogr. **52**, 850 (1996).
[15] S. Amelinckx, W. Luyten, T. Krekels, G. Van Tendeloo, and J. Van Landuyt, J. Cryst. Growth **121**, 543 (1992).
[16] L. Bourgeois, Y. Bando, S. Shinozaki, K. Kurashima, and T. Sato, Acta Crystallogr., Sect. A: Found. Crystallogr. **55**, 168 (1999).
[17] W. Q. Han, L. Bourgeois, Y. Bando, K. Kurashima, and T. Sato (unpublished).
[18] W. Q. Han, Y. Bando, K. Kurashima, and T. Sato, Appl. Phys. Lett. **73**, 3085 (1998).
[19] A. Krishnan, E. Dujardin, M. M. J. Treacy, J. Hugdahl, S. Lynum, and T. W. Ebbesen, Nature (London) **388**, 162 (1997).
[20] W. Luyten, T. Krekels, S. Amelinckx, G. Van Tendeloo, D. Van Dyck, and J. Van Landuyt, Ultramicroscopy **49**, 123 (1993).
[21] M. Ge and K. Sattler, Chem. Phys. Lett. **220**, 192 (1994).